scientific reports

Check for updates

OPEN

Proinflammatory macrophage secretome enhances temozolomide sensitivity in glioblastoma via pSTAT3-mediated downregulation of DNA repair enzymes

Susana López-López[1,2], Beatriz Castro-Robles[1,3], Natalia García-Flores[1], María José M. Díaz-Guerra[4], Lourdes Arias-Salazar[1,3], Hernán Sandoval[5], Daniel García-Pérez[5], Christoph J. Klein-Zampaña[5], Rosa A. Barbella-Aponte[6], Tomás Segura[3,4,7]✉ & Gemma Serrano-Heras[1,3]✉

The mechanisms by which tumor-associated macrophages, key components of the glioblastoma (GBM) microenvironment, impair chemotherapy efficacy remain poorly understood. Resistance to temozolomide (TMZ), the standard chemotherapeutic agent for GBM, is associated with poor prognosis due to efficient DNA repair mechanisms. While low expression of the DNA repair enzyme O6-methylguanine-DNA methyltransferase (MGMT) has been linked to improved TMZ response, our previous findings suggest that N-methylpurine-DNA glycosylase (MPG) may also contribute to chemoresistance in GBM. Here, we report for the first time that conditioned medium from pro-inflammatory macrophages (CM-M1) enhances TMZ cytotoxicity by suppressing STAT3 phosphorylation, resulting in decreased MGMT and MPG expression in GBM cells. Proteomic profiling of CM-M1 revealed a unique, cytokine-rich secretome that may promote STAT1 activation, thereby inhibiting pSTAT3 and reducing DNA repair enzymes levels. Clinically, elevated MGMT and MPG protein levels were associated with increased pSTAT3 in our GBM patient cohort, and analysis of the TCGA database further showed that their combined overexpression correlates with significantly reduced progression-free survival. Gene silencing experiments confirmed the contribution of both enzymes to TMZ resistance, with dual knockdown producing a synergistic sensitizing effect. These findings uncover a novel mechanism of macrophage secretome–mediated chemoresistance and support the development of M1-based strategies to improve TMZ efficacy in GBM.

Keywords Glioblastoma (GBM), Chemoresistance, Proinflammatory macrophage, Secretome, DNA repair enzymes, MPG

Glioblastoma (GBM) is the most common and aggressive malignant brain tumor in adults, with less than 5% of patients surviving beyond 5 years[1]. Standard treatment includes surgical resection, radiotherapy, and temozolomide (TMZ) chemotherapy, which improves survival[2]. However, TMZ resistance remains a major challenge. In recent years, tumor-associated macrophages (TAMs), the most abundant cells in the GBM microenvironment, have attracted considerable interest due to their role in promoting tumor growth, metastasis, and resistance to conventional therapies[3]. Macrophages polarize into two phenotypes: M1, which

[1]Research Unit, General University Hospital of Albacete, Laurel, s/n, 02008 Albacete, Spain. [2]School of Agricultural, Forestry and Biotechnology Engineering (ETSIAMB), University of Castilla-La Mancha (UCLM), Albacete, Spain. [3] Grupo de enfermedades cerebrovasculares, neurodegenerativas y neuro-oncológicas, Instituto de Investigación Sanitaria de Castilla-La Mancha (IDISCAM), Albacete, Castilla-La Mancha, Spain. [4]Medical School, Biomedicine Institute (IB), University of Castilla-La Mancha (UCLM), Albacete, Spain. [5]Department of Neurosurgery, General University Hospital of Albacete, Hermanos Falcó, 37, 02008, Albacete, Spain. [6]Department of Surgical Pathology, General University Hospital of Albacete, Hermanos Falcó, 37, 02008, Albacete, Spain. [7]Department of Neurology, General University Hospital of Albacete, Hermanos Falcó, 37, 02008 Albacete, Spain. ✉email: tseguram@gmail.com; gemmas@sescam.jccm.es

secrete proinflammatory cytokines (e.g., IL-1, CXCL10, TNF-α), and M2, which produce anti-inflammatory cytokines like IL-10. TAMs in GBM typically exhibit an M2-like, pro-tumoral profile, while M1 macrophages exert antitumor effects[4]. M2 macrophages have been described to promote chemoresistance by activating anti-apoptotic pathways such as STAT3 and BCL2, whereas M1 macrophages trigger STAT1-mediated apoptosis[5–9].

TMZ causes damage to cells through methylation at several nitrogenous bases in DNA, with the primary site of methylation occurring at the N7-guanine position (70%), followed by the N3-adenine position and at the O6-guanine residue (5%). However, the cytotoxic effect of TMZ in GBM cells becomes limited by the action of cellular DNA damage repair systems, which represent one of the main factors contributing to chemoresistance. It is well-established in the literature that elevated levels of MGMT, a DNA repair enzyme that removes the O6-methylguanine lesion, one of the most lethal lesions induced by TMZ, are a key factor driving TMZ resistance. Several studies conducted in patients treated with TMZ have reported that MGMT promoter methylation, leading to a lack of expression of the enzyme, is associated with improved overall survival compared to unmethylated GBM[10]. Nevertheless, a considerable proportion of patients fail to respond to TMZ treatment and do not exhibit clinical improvement even when the tumor expresses low levels of MGMT, suggesting that this DNA repair enzyme is not the only predictor of response to TMZ. In this context, previous findings from our group and others have highlighted the role of MPG, the initial enzyme in the base excision repair pathway (BER), in conferring TMZ chemoresistance in GBM[11,12]. MPG removes the most frequent TMZ-induced damages (N7-methylguanine and N3-methyladenine), leading to the formation of different intermediate adducts that are subsequently removed by downstream enzymes such as apurinic/apyrimidinic (AP) sites endonuclease 1 (APE1) and poly(ADP-ribose) polymerase (PARP), with the repair process finalized by DNA polymerase, POL-β. Consistently, the contribution of the base excision repair (BER) pathway, in which N-methylpurine-DNA glycosylase (MPG) acts as an initiating enzyme, to chemoresistance is supported by studies showing that pharmacological inhibition of downstream proteins such as APE1, PARP, and poly(ADP-ribose) glycohydrolase (PARG) enhances TMZ-induced cytotoxicity, regardless of MGMT expression[13–15].

It is worth noting that the interplay between the innate immune system and DNA repair pathways in GBM, as well as the transcription factors involved in their modulation, particularly in the context of chemoresistance, remains largely unexplored. One of the few studies that partially addresses this connection, conducted by Kohsaka et al.[16], revealed that STAT3 activation, which is frequently observed in tumors including GBM, upregulates MGMT expression. This suggests that the STAT3 signaling pathway may contribute to resistance to temozolomide (TMZ).

In this context, the present study aimed to gain insight into immune–tumor dynamics by investigating how macrophage-derived paracrine signaling influences the two DNA repair pathways associated with chemoresistance in GBM. Specifically, we examined the impact of conditioned medium from proinflammatory macrophages (CM-M1), a phenotype described as potentially exerting antitumor functions, on TMZ response, as well as its effect on the expression of the DNA repair enzymes MGMT and MPG in an in vitro GBM model. Furthermore, we investigated the regulatory mechanisms through which the CM-M1 secretome modulates the protein levels of these enzymes, with particular emphasis on the activation of the transcription factors STAT1 and STAT3. To identify unique secreted proteins potentially mediating these effects via modulation of pSTAT1 and pSTAT3, we performed liquid chromatography coupled with tandem mass spectrometry (LC-MS/MS) using SWATH acquisition. As a clinical approach, we evaluated associations between protein levels of MGMT, MPG, pSTAT1, and pSTAT3 in tumor samples from a cohort of 15 patients diagnosed with GBM. Additionally, in silico analyses of the TCGA database were conducted to assess correlations between DNA repair enzyme expression and patient prognosis, focusing on overall and progression-free survival in TMZ-treated individuals. Finally, to validate the combined activity of MGMT and MPG in promoting chemoresistance, siRNA-mediated silencing of these genes was performed.

Results

TMZ resistance, expression profile of DNA repair enzymes and activation of STAT1/3 in a GBM in vitro model

Viability assays performed on A172 and T98G glioblastoma cell lines incubated with increasing concentrations of TMZ for 72 h demonstrated a dose-dependent reduction in cell survival following TMZ treatment (Fig. 1A). The results indicated that both cell lines exhibited resistance to the chemotherapeutic agent, as high doses (400 µM) reduced cell viability by less than 50% (40% in A172 and 20% in T98G). BER pathway enzymes (MPG, APE1, PARP, and POL-β) and the mismatch repair (MMR) enzymes MSH2 and MSH6 were highly expressed in both GBM cell lines (Fig. 1B). While MGMT expression was absent in A172 cells, it was detected in T98G cells (Fig. 1B), potentially explaining the greater resistance observed in T98G cells (Fig. 1A). Furthermore, our findings align with previous studies reporting that A172 cells possess wild-type p53, whereas T98G cells harbor a mutated form of p53. This mutation disrupts normal protein degradation regulation, resulting in increased protein accumulation (Fig. 1B). Such alterations may partly account for the elevated MGMT levels in T98G cells, as mutated p53 has been reported to upregulate MGMT expression[17]. Although the lack of active MGMT, along with high levels of MSH2 and MSH6, is generally considered a sensitizing factor for TMZ treatment, our results suggest that the chemoresistance observed in A172 cells may be driven by other factors, such as enzymes involved in the BER pathway. In addition, total and activated (phosphorylated) levels of STAT1 and STAT3, were analyzed in GBM cells. As shown in Fig. 1B, both GBM cell lines exhibited elevated levels of phosphorylated Tyr705-STAT3, with T98G exhibiting the highest expression, while the activated form of STAT1 was found to be lower in T98G compared to A172 (Fig. 1B).

In summary, the A172 and T98G GBM cell lines displayed similarly high chemoresistance and activation of transcription factors potentially involved in macrophage-mediated signaling, while presenting distinct DNA repair enzyme profiles.

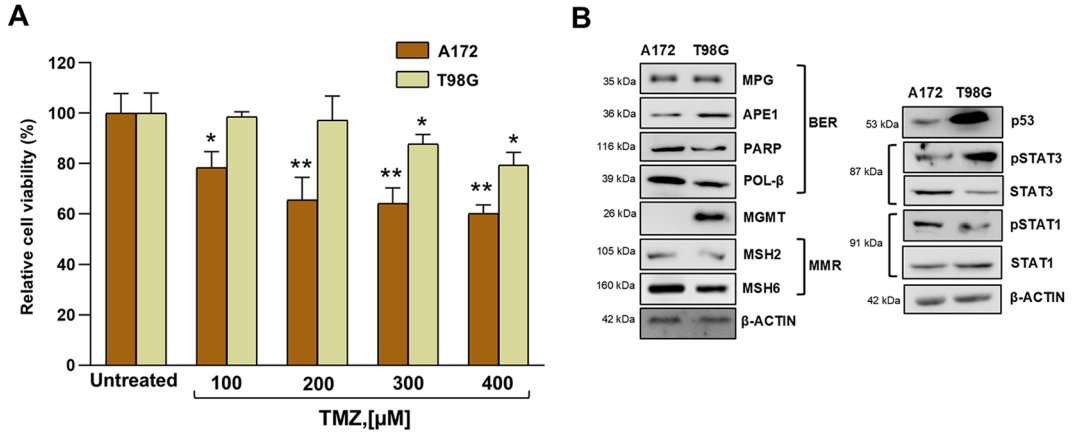

Fig. 1. Repair mechanisms of DNA damage in TMZ-resistant GBM cell lines. (**A**) A172 and T98G cells were cultured for 5 days with different TMZ concentrations and chemoresistance was evaluated by MTT assay. Cell viability was normalized to untreated cells (mean ± SD from three independent experiments). Mann-Whitney U or Student's t-test: $^{*}p < 0.05$ or $^{**}p < 0.01$ versus untreated. (**B**) Western blot (representative image from three experiments) of BER, MGMT, MMR repair pathways, p53 and total and phosphorylated STAT3 and STAT1, with β-actin as loading control (original blots are presented in supplementary material: Figure s1).

Conditioned medium from proinflammatory macrophages potentiates TMZ efficacy in GBM cells by reducing cell viability and inducing apoptotic cell death

We sought to examine whether conditioned media containing proteins secreted by polarized M1 and/or M2 macrophages affect TMZ efficacy in an in vitro GBM model.

To this end, macrophages underwent an activation and differentiation process, as described in the Methods section, to collect unconditioned medium (UC-M), corresponding to the medium prior to activation and differentiation; conditioned medium collected during macrophage activation without differentiation (CM-M0); and conditioned medium obtained during the differentiation of activated macrophages into either proinflammatory (M1) or anti-inflammatory (M2) phenotypes. M1 differentiation was confirmed by measuring STAT1 phosphorylation, a key transcription factor in pro-inflammatory activation, and by detecting increased expression of the pro-inflammatory genes TNFα and CXCL-10 compared to M0 or M2 macrophages (Fig. 2A). However, M2 markers such as Arg1 and IL-10 were only modestly induced, consistent with previous studies showing that THP-1-macrophage cells do not fully differentiate into the M2 phenotype (Fig. 2A). As a result, subsequent experiments were conducted using UC-M and CM-M0 as controls, while only the conditioned medium from M1 macrophages (CM-M1) was used for treatment. Nonetheless, this approach enabled us to explore the influence of macrophage-derived paracrine signaling on TMZ response in GBM.

We first analyzed the effect of CM-M1 on the viability of GBM cell lines under TMZ treatment to determine whether this proinflammatory medium enhances chemosensitivity. Cell viability was assessed after incubating the cells with UC-M, CM-M0, or CM-M1 for 24 h, followed by an additional 72 h in the presence or absence of TMZ. Our results showed that exposure to CM-M1, but not to the other media, significantly reduced cell viability in both cell lines (Fig. 2B), which could be partially attributed to the downregulation of BCL2 (Fig. 2C), an anti-apoptotic gene. More interestingly, incubation with CM-M1 combined with low-dose TMZ treatment (100 μM in A172 and 300 μM in T98G) led to a significantly greater reduction in cell survival compared to treatment with either the inflammatory medium or the chemotherapeutic agent alone (Fig. 2B).

Subsequently, GBM cell death induced by exposure to CM-M1 alone or in combination with TMZ was analyzed by flow cytometry. We found that apoptosis was synergistically increased by the combination of proinflammatory macrophage medium and TMZ, with a higher percentage (5.4 ± 0.3% and 17.2 ± 1%) of A172 cells undergoing early and late apoptosis, respectively, compared to 4.5 ± 0.1% and 12.7 ± 2%, or 4.4 ± 0.2% and 14.7 ± 1.5%, in the individual CM-M1 and TMZ treatment groups (Fig. 2D). Similar results were observed in T98G cells, with 40.3 ± 2.7% total apoptotic cells, in comparison to 35.2 ± 1.8% and 17.3 ± 4% after separate incubation with M1 medium and chemotherapy agent (Fig. 2D). These findings were further supported by western blot analysis, which showed increased levels of the pro-apoptotic protein cleaved Caspase-3 in the combined treatment group (Fig. 2E).

Taken together, these results suggest that CM-M1 potentiates the deleterious effects of TMZ by triggering apoptosis, which, in synergy with chemotherapy, leads to an increased number of cells undergoing cell death via apoptosis.

M1 macrophages-derived medium inhibits MGMT and MPG expression in GBM cells through blocking pSTAT3 signaling

Next, we aimed to characterize the molecular mechanisms underlying the sensitization of GBM cell lines to TMZ induced by the M1 macrophage secretome. Specifically, we examined the protein levels of MPG and MGMT, as well as STAT3, STAT1, and their phosphorylated forms, in T98G and A172 cells after incubation with CM-M1 and control media from non-activated macrophages (UC-M) and activated but non-differentiated macrophages

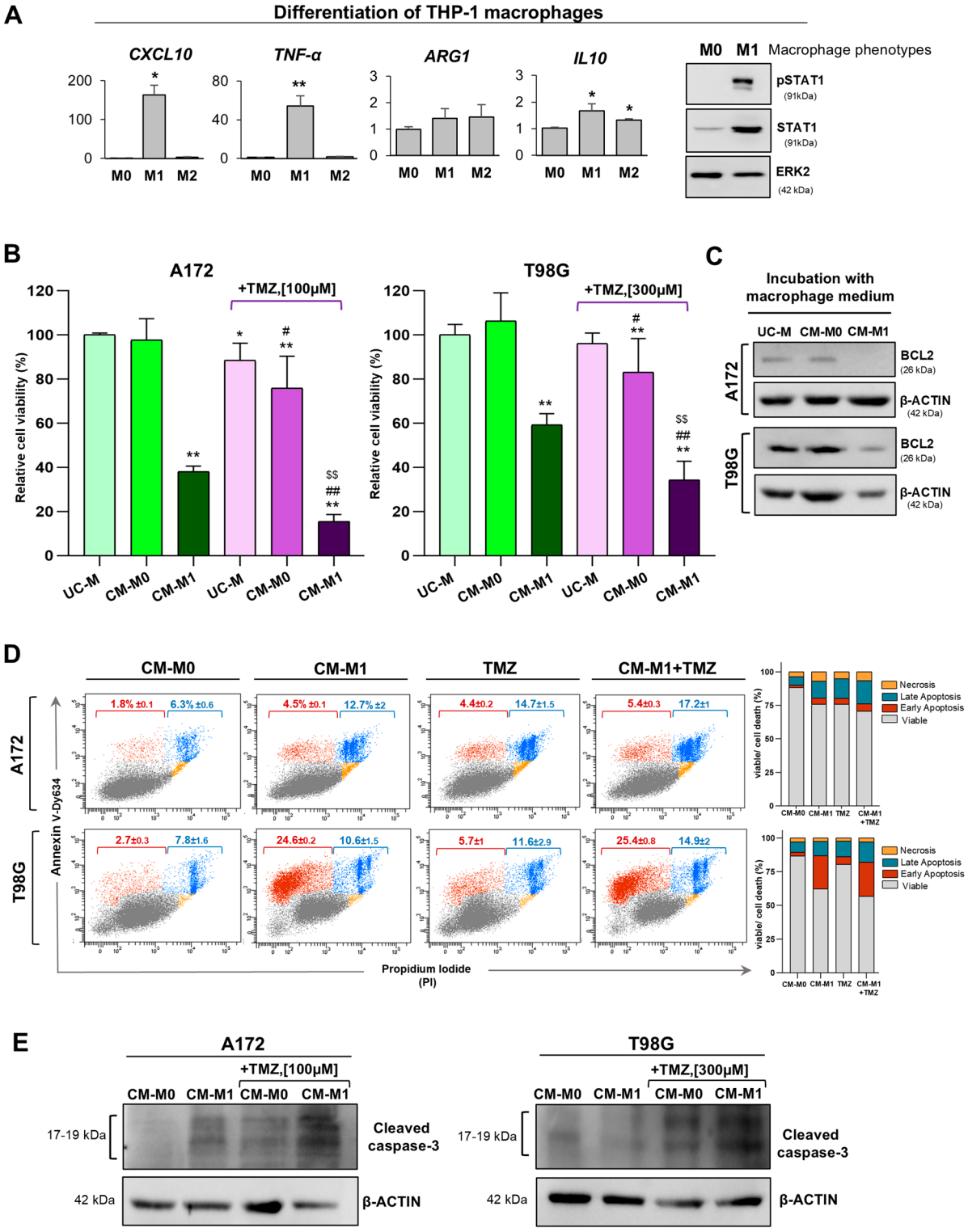

(CM-M0). CM-M1-treated GBM cells exhibited reduced levels of the activated (phosphorylated) form of STAT3, which functions as a transcription factor, compared to cells treated with UC-M and CM-M0, while total STAT3 protein levels remained largely unchanged. In contrast, CM-M1 exposure triggered an increase in both STAT1 activation (phosphorylation) and expression (total protein levels) (Fig. 3A) Additionally, we observed a reduction in the expression of the DNA repair enzymes MPG and MGMT following incubation with M1 proinflammatory medium, relative to cells exposed to UC-M and CM-M0 (Fig. 3A).

To determine whether the M1 macrophage–conditioned medium mediates the downregulation of DNA repair enzymes through transcription factor signaling, GBM cells were transfected with STAT1 or STAT3 overexpression vectors to assess whether the observed reduction in MPG and MGMT expression was directly linked to decreased pSTAT3 or increased pSTAT1 levels. Forced STAT1 expression and the resulting increase in pSTAT1 did not lower MPG or MGMT levels compared to control cells transfected with an empty vector. In

◀**Fig. 2**. Enhanced TMZ cytotoxicity by M1 medium through the induction of apoptosis and suppression of BCL-2. (**A**) mRNA expression of markers associated with the pro-inflammatory M1 phenotype (CXCL-10, TNF-α) and the anti-inflammatory M2 phenotype (Arg1, IL-10) was analyzed by qRT-PCR and normalized to GAPDH mRNA following the differentiation of THP-1 macrophages (mean ± SD from three independent experiments). Student's t-test: $^{*}p < 0.05$ or $^{**}p < 0.01$ compared to M0 (non-polarized macrophages). Western blot analysis was used to assess STAT1 expression and activation in proinflammatory macrophages (M1). (**B**) GBM cell viability was assessed in cells cultured in unconditioned medium (UC-M) or in conditioned medium derived from either non-differentiated (CM-M0) or M1-differentiated (CM-M1) macrophages, followed by incubation with or without temozolomide (TMZ), using the MTT assay. Cell viability was normalized to untreated cells incubated in unconditioned medium (UC-M) (mean ± SD from three independent experiments). one-way ANOVA test: * or ** versus UC-M TMZ-untreated cells and TMZ-untreated cells incubated in CM-M0 and CM-M1; # or ## indicate comparisons between the same medium with and without TMZ treatment; $$ versus UC-M TMZ-treated cells and TMZ-treated cells incubated in CM-M0 and CM-M1 ($p < 0.05$ or $p < 0.01$). (**C**) BCL2 anti-apoptotic protein expression was evaluated by Western blot ($n = 3$) in A172 and T98G cells incubated with unconditioned or M0 or M1 conditioned medium. (**D**) Representative flow cytometry dot plot ($n = 2$) showing cell death by early (brown dots) and late (blue dots) apoptosis, and necrosis (orange dots) in cells treated under different conditions, using Annexin V-Dy634 and PI staining. (**E**) After treatment with M0/M1 conditioned medium and/or TMZ, cleaved caspase-3 levels were analyzed by Western blot ($n = 3$). β-actin was used as a loading control. Original blots are presented in supplementary material: Figures s2 and s3.

contrast, STAT3 overexpression, which led to elevated levels of its phosphorylated form, significantly increased the expression of both enzymes (Fig. 3B). Next, we used a selective STAT3 inhibitor that completely abolished STAT3 phosphorylation[18], resulting in decreased MGMT and MPG expression (Fig. 3C). Finally, to confirm that the CM-M1-induced downregulation of MGMT and MPG is mediated by pSTAT3, GBM cells, either transfected with an empty vector or overexpressing STAT3, were incubated with the proinflammatory medium. As shown in Fig. 3D, STAT3 overexpression and the associated increase in pSTAT3 substantially attenuated the CM-M1-induced suppression of DNA repair enzyme expression.

Our findings demonstrate that proinflammatory conditioned medium suppresses MGMT and MPG expression in GBM cells by inhibiting pSTAT3 signaling, highlighting the role of macrophage-secreted factors regulating STAT3 in DNA repair mechanisms in GBM. These results may help explain the enhanced apoptotic response previously observed (Fig. 2B–E) following combined treatment of GBM cells with the proinflammatory medium and TMZ. This effect could be partly attributed to increased STAT1 activation, a known negative regulator of cell proliferation and promoter of apoptotic signaling. Moreover, considering that previous studies have reported reciprocal negative cross-regulation between STAT1 and STAT3[19], the STAT1 activation induced by CM-M1 may also inhibit pSTAT3, ultimately leading to the downregulation of MGMT and MPG.

Proteomic analysis of the M1 macrophage secretome reveals a distinct proinflammatory signature with potential inhibitory effects on STAT3 activation

To identify candidate proteins secreted by M1 macrophages that may modulate STAT1/3 signaling, we performed quantitative proteomic analysis using LC-MS/MS with SWATH acquisition on unconditioned medium and conditioned media from M0 and M1 macrophages (two replicates each). A total of 522 soluble proteins were identified, with 73% shared across all media, 17% between CM-M0 and CM-M1, and 49 unique to CM-M1 (Fig. 4A, supplementary material: Proteomic data file). Principal component analysis (PCA) based on 327 features revealed clear separation among the three conditions, with PC1 and PC2 explaining 74.2% and 14.1% of the variance, respectively, highlighting the distinct proteomic profile of CM-M1.

To explore the functional relevance of CM-M1–specific proteins, we conducted enrichment and protein–protein interaction (PPI) analyses. The most significant enrichment (FDR = 1×10^{-4}) was observed for cytokine/chemokine activity, receptor binding, and RNA binding (Fig. 4B). The PPI network (Fig. 4C) revealed four clusters, including a core of cytokines and chemokines such as TNF and IL-1β, known to enhance STAT1 activation and apoptosis[8,19,20]. Elevated pSTAT1 may promote cell death and suppress STAT3 signaling, reducing MGMT and MPG expression and increasing chemosensitivity. This cluster also includes CXCL10 and CXCL9, which, through binding to the CXCR3-B isoform in GBM, may suppress proliferation and induce apoptosis independently of STAT1/3[21,22].

Two additional clusters were identified (Fig. 4C): one involving transcriptional regulators such as FUBP1, which can act as either oncogenic or tumor-suppressive depending on contex[23] and mRNA-binding proteins involved in post-transcriptional regulation (e.g., HNRNPM, HNRNPL, SNRPF, SNRPA, RBM3, RBM8A). Another compact module includes proteins related to protein synthesis (RPL14, RPLP1, RPS2) and nucleoside metabolism, including thymidine phosphorylase (TYMP). Interestingly, while TYMP can promote tumor growth, certain concentrations have been shown to enhance the cytotoxic effects of chemotherapy agents such as 5-fluorouracil (5-FU)[24].

Beyond CM-M1–exclusive proteins, 87 were differentially expressed between CM-M0 and CM-M1, with 77 upregulated in both M1 replicates (Fig. 4D). Of these, approximately 50% showed a > 2-fold increase ($\log_2 FC > 1$, p. value adjusted < 0.05, $\text{Log}_{10}\text{pAdj} > 1.3$; Fig. 4E). Enrichment analysis of these proteins revealed networks related to nucleic acid binding, gene expression, and protein synthesis (Fig. 4F).

In summary, this proteomic study reveals the presence of unique proteins secreted by macrophages polarized toward a proinflammatory phenotype, with potential cytotoxic effects on GBM cells. Furthermore, these

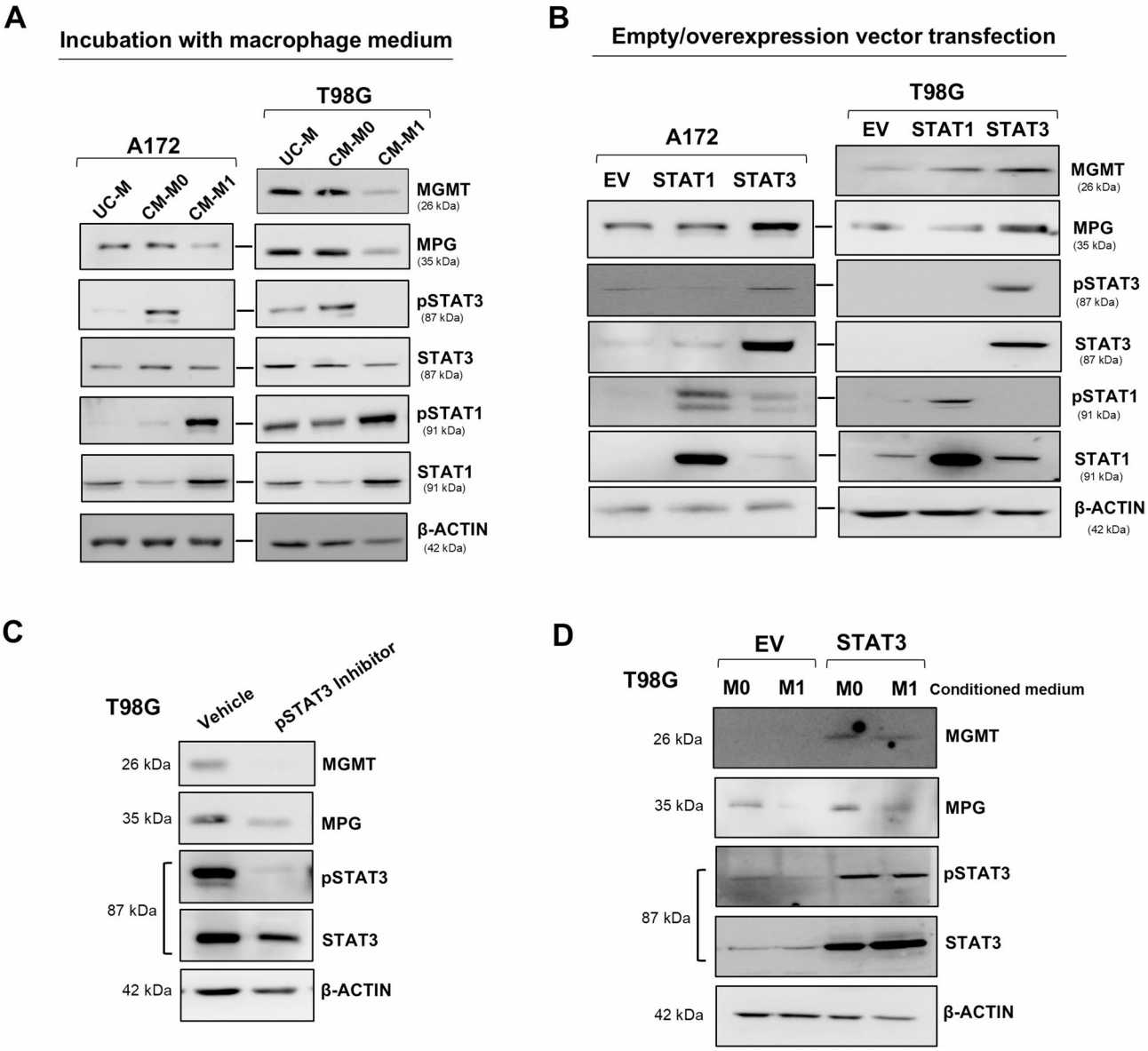

Fig. 3 Please make sure that Figure 3 is placed in the manuscript close to the Results section [M1 macrophages-derived medium inhibits MGMT and MPG expression in GBM cells through blocking pSTAT3 signaling], where it is cited, as we have seen in the PDF-proof that it is currently located far from that section. M1 macrophage-derived medium reduces MGMT and MPG expression in GBM cells by inhibiting STAT3 activation. (**A**) Effect of M1 macrophage medium (24-hour incubation) on STAT1/STAT3 activation and DNA repair enzymes (MGMT, MPG) was evaluated by Western blot. (**B**) Protein levels of DNA repair enzymes and transcription factors were analyzed in GBM cells transiently transfected with STAT1/STAT3 overexpression or empty vectors. (**C**) MGMT, MPG, p-STAT3, and STAT3 expression were analyzed in T98G cells treated with a STAT3 activation inhibitor. (**D**) Western blot analysis of MGMT and MPG in T98G cells transiently transfected with STAT3 or empty vectors, followed by treatment with conditioned medium from M1-differentiated or M0 control macrophages. Representative Western blots from three independent experiments, with β-actin as a loading control. Original blots are presented in supplementary material: Figures s4, s5 and s6.

exclusive CM-M1 proteins may contribute to the downregulation of pSTAT3 via increased pSTAT1, ultimately leading to reduced expression of DNA repair enzymes and enhanced sensitivity to TMZ.

MGMT and MPG expression and STAT3 activation in patient-derived GBM and their association with prognosis

As described above, our in vitro results indicate that pSTAT3 regulates the expression of DNA repair enzymes and that M2 macrophages, through modulation of this transcription factor, influence the response to TMZ in GBM. To translate these findings into a clinical context, we first investigated the potential correlation between

MGMT and MPG expression and pSTAT3 levels in GBM patient samples. Western blot analysis was performed on 15 tumor tissue samples obtained from patients diagnosed with glioblastoma who underwent tumor resection surgery. The median age of patients was 55 years (range: 40–78), with 40% being female. The time between diagnosis and surgery ranged from 0 to 45 days, with an average of 15.6 days. The majority of patients received a combination of radiation therapy and temozolomide (RT-TMZ + TMZ) as their first-line treatment, although some were treated with temozolomide alone or did not receive treatment. GBM recurrence (assessed through imaging studies, such as MRI, showing new tumor growth or changes 4 to 6 months after the completion of the first therapeutic regimen) was observed in 10 (67%) patients (GB1, 2, 6, 7, 8, 9, 10, 12, 13, 15).

The molecular results showed that 53% of patients ($n = 8$) expressed pSTAT3 (Fig. 5A). Among these, 87.5% ($n = 7$) exhibited MGMT expression, and 87.5% ($n = 7$) had detectable MPG protein levels. Notably, 75% of the pSTAT3-positive patients ($n = 6$) expressed both MGMT and MPG (Fig. 5A), suggesting that activated STAT3 may regulate the expression of these two DNA repair enzymes in patient tumors, consistent with our observations in the in vitro GBM model. We did not find a significant relationship between enzyme expression, transcription factor activation, and tumor relapse after treatment, probably due to the small sample size of our cohort.

Next, to validate our findings in a larger patient cohort, we performed in silico analyses using The Cancer Genome Atlas (TCGA), specifically the PanCancer Atlas dataset. This dataset includes 585 patients with glioblastoma, of whom 334 received temozolomide (TMZ) treatment and had available data on DNA repair enzymes and STAT3 activation. Since only mRNA expression data (z-scores) were available, rather than protein-level values, the protein correlations observed in our patient cohort by western blot (suggesting an association between MGMT and MPG levels and pSTAT3) could not be directly confirmed. However, we assessed the prognostic implications of MGMT and MPG upregulation, as well as STAT3 activation. Interestingly, high expression of MGMT, MPG, or both combined, as well as elevated pSTAT3, did not significantly correlate with overall survival (OS). Nonetheless, all these conditions were associated with a statistically significant, or near-significant, reduction in progression-free survival (PFS) compared to the control (unaltered) group (Fig. 5B). Median PFS in these subgroups was approximately 6 months, versus over 11 months in the control group, indicating a poorer prognosis. The highest hazard ratio (1.894) was observed in patients with high expression of both MGMT and MPG (Fig. 5B). This lack of association with OS, but significant link to shorter PFS, suggests that MGMT and MPG expression, together with STAT3 activation, may contribute to early tumor progression and resistance to initial chemotherapy, rather than long-term survival outcomes.

Increased GBM chemosensitivity through MPG silencing, both alone and synergistically with MGMT downregulation

To investigate the impact of both DNA repair enzymes on temozolomide (TMZ) efficacy, small interfering RNAs (siRNAs) were used to suppress MGMT and MPG expression. GBM cell lines were initially transfected with varying concentrations of MGMT- and MPG-targeting siRNAs, both individually and in combination, to determine the optimal conditions for achieving efficient reduction of enzyme expression at both the protein and mRNA levels. MPG expression was effectively inhibited in A172 cells using a siRNA concentration of 25 nM, whereas T98G cells required 40 nM for optimal inhibition (Supplementary Fig. s9), with maximum suppression observed 96 h post-incubation in both GBM cell lines (Supplementary Fig. s10, Supplementary Fig. s11, Supplementary Fig. s12, Fig. 6A). In T98G cells, which express both DNA repair enzymes, a 25 nM concentration of MGMT-targeted siRNA effectively reduced MGMT expression separately, and this peak effect was sustained when both enzymes were simultaneously knocked down 96 h after exposure to the specific siRNAs (Supplementary Fig. s10, Supplementary Fig. s12, Fig. 6A). The expression of enzymes involved in the subsequent steps of the MPG-mediated base excision repair (BER) pathway, as well as the MMR enzymes MSH2 and MSH6, was unaffected in the absence of MPG and MGMT (Fig. 6A). Additionally, siRNAs targeting these DNA repair enzymes remained effective even in the presence of TMZ (Fig. 6A).

It is worth mentioning that the optimal incubation time for gene silencing, set at 96 h, enabled the viability studies with TMZ-treated GBM cells, as it aligned with the experimental conditions. SiRNA typically requires approximately 48 h to take effect, while TMZ induces cell death over extended periods (see experimental protocol scheme, Fig. 6B). As shown in Fig. 6B, MPG siRNA significantly enhanced TMZ sensitivity in A172 cells, which do not express MGMT. Moreover, the combined inhibition of MPG and MGMT in TMZ-treated T98G cells resulted in a synergistic decrease in cell viability, with statistically significant differences compared to each siRNA treatment alone. Collectively, our results suggest that MPG activity, either alone or in combination with MGMT, plays a significant role in contributing to TMZ resistance in GBM.

Discussion

Chemoresistance in GBM occurs frequently, and one contributing factor is the presence of M2 macrophages in the tumor microenvironment[25–28], highlighting the need for further investigation into the molecular mechanisms by which tumor-associated macrophages drive resistance in GBM. This study provides, to the best of our knowledge, the first evidence that proinflammatory conditioned medium derived from M1 macrophages induces a pSTAT3-dependent downregulation of the DNA repair enzymes MGMT and MPG, thereby enhancing GBM cells' sensitivity to TMZ and improving chemotherapy effectiveness. In agreement, previous research has demonstrated that blocking STAT3 phosphorylation decreases the IC50 of TMZ in GBM cells, enhancing TMZ-induced apoptosis, partly through reduced BCL-2 expression, a downstream target of p-STAT3[16]. Thus, our study demonstrates for the first time that pSTAT3 modulates the expression of both MPG and MGMT. This finding aligns with tumor analyses from patients, which show higher expression of both enzymes in pSTAT3-positive samples (75%) compared to those lacking activated STAT3. Very interestingly, proteomic analysis identified a unique proinflammatory cytokine and chemokine signature in the M1 secretome with the potential to induce STAT1 activation. Since pSTAT1 negatively regulates pSTAT3 transcriptional function[19], the increase

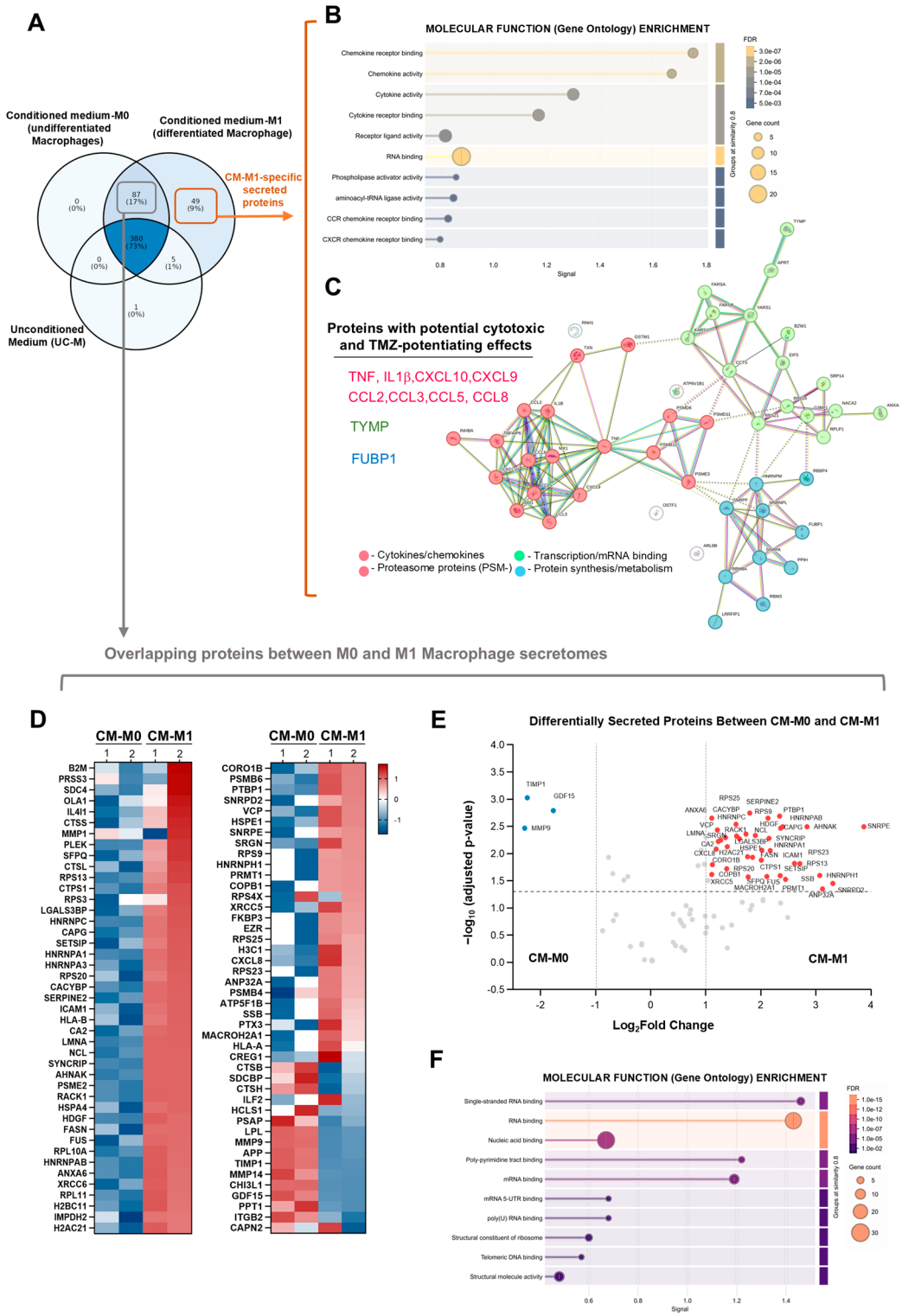

in pSTAT1, induced by specific proinflammatory proteins secreted by M1 macrophages, could suppress pSTAT3 activity, leading to downregulation of DNA repair enzymes and, ultimately, potentiating chemotherapy efficacy, as illustrated in Fig. 7. This visual representation of the novel mechanism by which macrophages lead to TMZ sensitization in GBM also includes a possible pathway through which the proinflammatory medium, even in the absence of chemotherapeutic treatment, triggers a reduction in GBM cell viability and the induction of apoptosis (Fig. 2B–E). These effects are comparable to those previously reported in breast cancer cell cultures[29] and renal clear cell carcinoma[30] treated with CM-M1. The impaired cell survival and increased apoptosis may be attributed to the upregulation of the phosphorylated form of STAT1. The antiproliferative and proapoptotic role of pSTAT1 has been previously described and involves both transcription-dependent and transcription-independent mechanisms of cell death regulation[5,6,8]. The transcription-dependent mechanism activates genes involved in death modulation and cell-cycle arrest (e.g., caspases, death receptors, iNOS, Bcl-xL, p21), while the

◂**Fig. 4 Please make sure that Figure 4 is placed in the manuscript close to the Results section [Proteomic analysis of the M1 macrophage secretome reveals a distinct proinflammatory signature with potential inhibitory effect on STAT3 activation], where it is cited, as we have seen in the PDF-proof that it is currently located in Discussion section**. Identification of M1-specific secreted proteins as candidate paracrine signals for pSTAT3 downregulation in GBM using quantitative proteomics and bioinformatic analysis. (**A**) Venn diagram showing the overlap and number of unique proteins identified in UC-M, CM-M0, and CM-M1 media, including their respective proportions relative to the total proteins detected. (**B**) Gene Ontology analysis of Biological Process pathway enrichment for the 47 proteins specifically identified in the secretome of pro-inflammatory macrophages. Each dot represents a significantly enriched GO term, grouped by functional similarity. Dot size indicates the number of associated proteins, while the x-axis reflects the enrichment score. Color intensity represents the false discovery rate (FDR), ranging from dark blue (lowest FDR) to grey and yellow (higher FDR). (**C**) Proteins with potential cytotoxic effects via apoptosis induction and enhancement of TMZ efficacy, resulting from increased STAT1 activation and pSTAT3 inhibition in GBM. A protein–protein interaction (PPI) network was constructed from M1-specific secreted proteins using the STRING database. Nodes represent proteins; edges represent known or predicted interactions. Line thickness reflects interaction confidence. Proteins are colored according to four functional clusters: two red subnetworks representing cytokines/chemokines and proteasome-related proteins; one green network comprising transcription/mRNA-binding proteins; and a core cluster involved in protein synthesis and metabolism. (**D**) Heatmap of proteins shared between M0 and M1 secretomes. It displays z-score normalized expression levels of 87 overlapping proteins across medium samples. Each row corresponds to a protein, and each column to a replicate of CM-M0 or CM-M1. Color intensity reflects relative abundance, with red tones indicating increased secretion and cooler tones indicating lower secretion. (**E**) Volcano plot showing differentially secreted proteins between CM-M0 and CM-M1. Each dot represents a protein, positioned by log2 fold change (x-axis) and –log10 adjusted *p*-value (y-axis). Dashed vertical lines indicate fold change thresholds (log2FC ± 1), and the horizontal dotted line marks a –log10(p-value) of 1.3 ($p < 0.05$). Proteins with significant changes are highlighted in red (increased secretion in CM-M1, $n = 39$) or blue (decreased secretion in CM-M1, $n = 3$). (**F**) Molecular function enrichment analysis of significantly upregulated proteins in M1-conditioned medium.

transcription-independent mechanisms rely on pSTAT1 interactions with apoptosis-related proteins such as TRADD, p53, and HDAC[6].

It is worth noting that protein secretion is a key mechanism by which macrophages modulate their surrounding microenvironment. In recent years, advanced mass spectrometry-based secretomics has been increasingly employed to characterize macrophage secretomes, revealing distinct secretory profiles that influence both immune and non-immune cells, including tumor cells, through paracrine signaling[31,32]. In our study, M1 macrophage secretome profiling revealed a distinct molecular signature comprising four functional clusters. The main group included proinflammatory cytokines and chemokines, mostly secreted via classical pathways, although some may be associated with extracellular vesicles. Additional clusters involved components of the proteasome, proteins related to metabolism and translation, and transcriptional regulators, likely present in the medium via extracellular vesicles or as a result of cell lysis. Among the candidates with potential cytotoxic and/or chemosensitizing effects via downregulation of DNA repair enzymes, proinflammatory cytokines such as TNF-α and IL-1β stand out. Both have been associated with increased STAT1 activation and the induction of apoptosis[8,19,20]. As discussed earlier, elevated pSTAT1 levels would promote cell death and inhibit STAT3 activation, thereby reducing DNA repair enzyme expression and enhancing TMZ sensitivity (as illustrated in Fig. 7). Notably, we also identified CXC chemokines such as CXCL9 and CXCL10, which, through the CXCR3 receptor, expressed in GBM, have shown antiproliferative and pro-apoptotic effects via STAT-independent pathways[21,22]. Furthermore, CM-M1 contained CC chemokines (CCL2, CCL3, CCL5, and CCL8), which are known to support tumor progression and cell cycle activation in GBM[33]. We hypothesize that elevated levels of these ligands may saturate CCR receptors on GBM cells, triggering receptor internalization via clathrin-mediated endocytosis, as previously described for CCR5[34].

Finally, in this study, we performed siRNA-mediated knockdown of MGMT and MPG with the aim of functionally validating their dual involvement in driving resistance to TMZ. For more than a decade, chemoresistance in GBM has been largely attributed to MGMT, which repairs the most cytotoxic TMZ-induced DNA lesions. Indeed, the methylation status of the MGMT promoter, leading to low MGMT expression, was the first molecular marker used to predict a better response to TMZ in clinical trials[35]. However, data showing that chemotherapy-induced cytotoxicity persists even in the absence of MGMT have highlighted the MPG-initiated BER pathway as a potential complementary mechanism contributing to chemoresistance. In recent years, however, there has been controversy regarding its role, as this DNA repair pathway has been associated with both promoting resistance and enhancing TMZ efficacy. On the one hand, high MPG expression has been associated with poorer prognosis in glioma patients[12,36], consistent with our in silico analysis using the TCGA database, which showed a hazard ratio of 1.456 for patients with high MPG expression, slightly lower than the risk associated with high MGMT expression (HR = 1.713). In both groups, reduced progression-free survival was observed, with median overall survival just over 6 months, compared to nearly 11 months in patients without elevated levels of either enzyme. In the same line, it has been observed that, in some glioblastoma patients, resistance to TMZ cannot be fully explained by MGMT promoter methylation alone, suggesting that MPG may play an additional role in mediating chemoresistance[37]. Other studies have further shown that the expression of MPG and POL-β predicts sensitivity to chemotherapeutic agents[38], and that reduced expression of BER proteins, such as APE1 and PARP, via chemical inhibitors sensitizes GBM cells to TMZ[13,14]. On the other hand, Fosmark

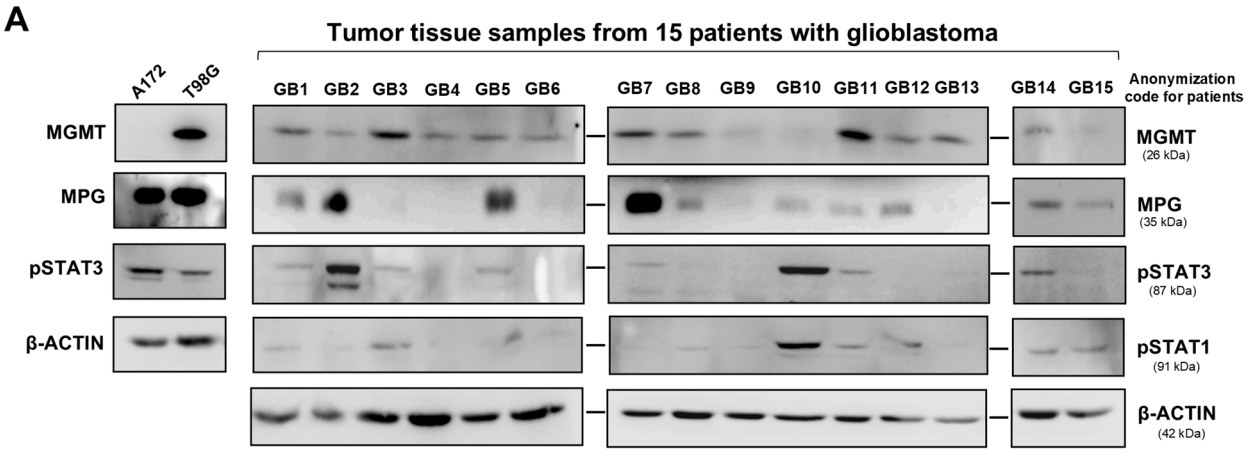

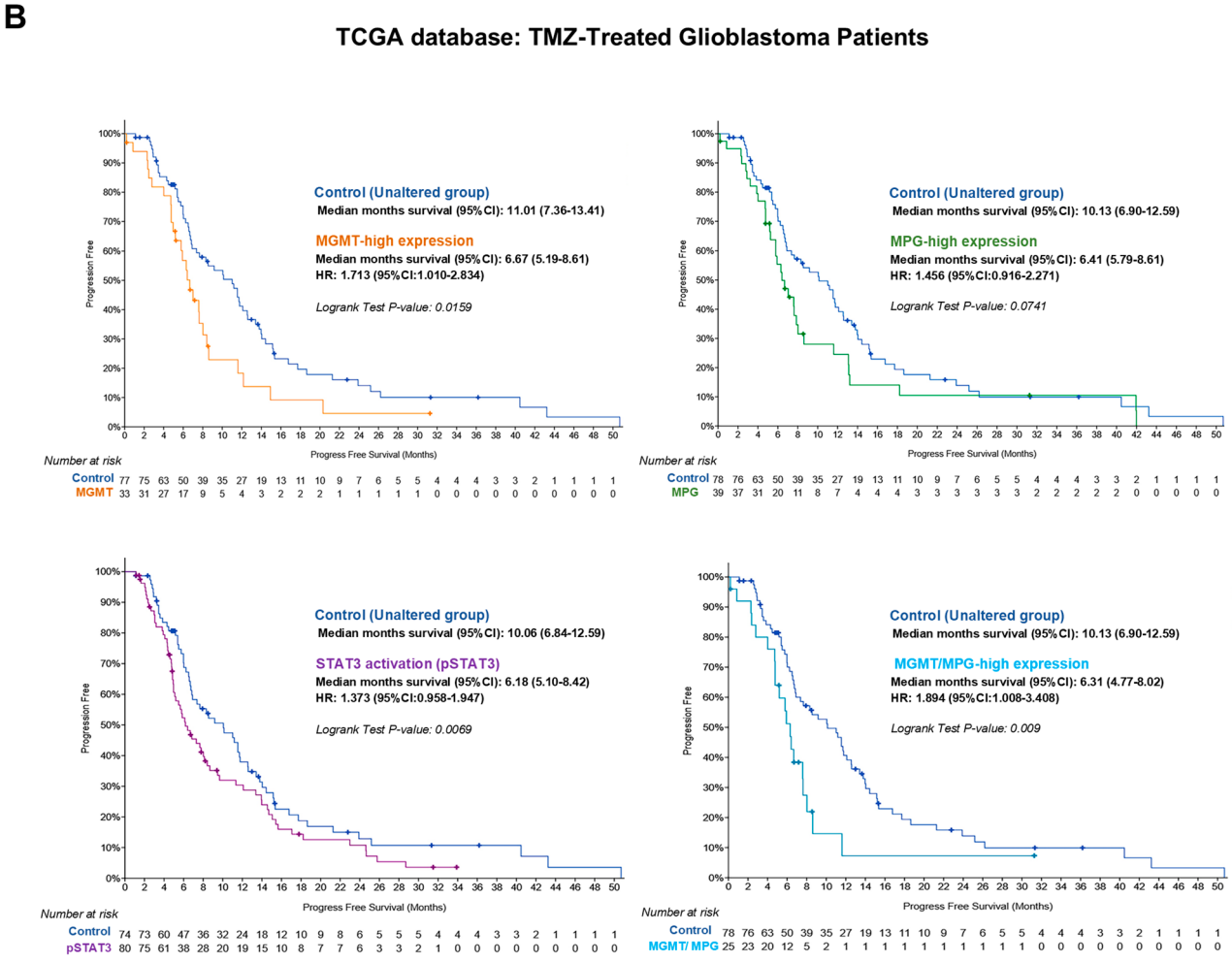

et al.[39] reported that high MPG expression correlated with improved survival in glioblastoma patients with MGMT promoter methylation. Additional evidence suggesting that elevated MPG levels may enhance TMZ efficacy, rather than contribute to chemoresistance, in GBM and other cancers comes from studies combining MPG overexpression with inhibition of downstream BER enzymes, such as APE1 and PARP[38,40]. This increased sensitivity was attributed to the accelerated repair of N-methylpurine lesions by MPG, which overwhelmed the rate-limiting enzyme POL-β and led to the accumulation of cytotoxic 5'-dRP repair intermediates. According to these findings, inhibition of downstream BER enzymes would enhance TMZ efficacy only under conditions of high MPG and low POL-β expression. In contrast, our study demonstrates that silencing MPG sensitizes GBM cells to TMZ in both MGMT-expressing (T98G) and MGMT-deficient (A172) cells, regardless of POL-β expression levels. This indicates that MPG plays a significant role in driving TMZ resistance. These results are consistent with our previous findings linking high MPG expression to TMZ-resistant phenotypes in patient-

◂**Fig. 5 Please make sure that Figure 5 is placed in the manuscript close to the Results section [MGMT and MPG expression and STAT3 activation in patient-derived GBM and their association with prognosis], where it is cites, as we have seen in the PDF-proof that it is currently located in the Discussion section**. Preferential expression of MGMT and MPG in glioblastoma patient samples with STAT3 activation and associated survival outcomes. (**A**) Western blot analysis ($n = 4$) of MGMT and MPG protein levels, as well as STAT3/STAT1 phosphorylation, in A172 and T98G cells and 15 patient-derived tumor samples. Original blots are presented in supplementary material: Figure s7. (**B**) Survival analysis of a glioblastoma cohort treated with TMZ from the TCGA dataset (334 patients) was conducted using the cBioPortal platform. Patients were classified into two groups based on high versus low expression or activation levels. Kaplan–Meier plots were generated to compare progression-free survival (PFS) among groups with high expression of MGMT, MPG, MGMT + MPG, and pSTAT3. The median mRNA expression levels of DNA repair enzymes or median phosphorylated protein levels were used as cutoffs to define high versus low expression or activation. Statistical significance between survival curves was assessed using the log-rank test.

derived GBM cells[11]. Interestingly, simultaneous knockdown of both DNA repair enzymes revealed that MPG acts synergistically with MGMT to limit TMZ efficacy. This cooperative interaction is further supported by our TCGA analysis, which showed that patients with high expression of both enzymes experienced a more pronounced reduction in progression-free survival compared to groups exhibiting elevated levels of either enzyme alone.

Together, our findings unveil the underlying mechanisms by which macrophage-secreted factors within the GBM microenvironment may influence the response to TMZ through the modulation of DNA repair enzyme expression. These results support strategies aimed at enhancing the activity of the M1 macrophage phenotype, either through local application of proinflammatory secretomes or by reprogramming M2 macrophages into an M1 phenotype, as adjuvant approaches to improve chemotherapy response in GBM. This approach could also serve as an alternative to current immunotherapies focused on enhancing adaptive immunity[41], which have shown limited efficacy in GBM[42]. Indeed, various compounds, including corosolic acid[43] and inhibitors of placental growth factor, C/EBPβ (CCAAT/enhancer-binding protein beta), and the hyaluronic acid pathway, have demonstrated efficacy in reprogramming macrophages from the M2 to the M1 phenotype in GBM, resulting in tumor suppression through STAT3 inhibition[44,45]. We suggest that an M1-based strategy to block DNA repair systems may be a better option than the development of synthetic MPG or MGMT inhibitors. To date, targeting MPG has been unsuccessful due to the complexity of its active site. Unfortunately, pharmacological approaches targeting MGMT have also failed to significantly reduce chemoresistance in clinical trials, as they necessitated lowering TMZ doses to avoid severe myelosuppressive toxicity caused by inhibitors such as Lomeguatrib or PaTrin-2[46,47].

We acknowledge certain limitations of this study. First, the in vitro GBM cell models used in this study do not fully replicate the complex tumor microenvironment observed in glioblastoma patients. Although our molecular assays and secretome analyses indicate a paracrine role for macrophages in modulating chemoresistance in GBM, aligning with the established notion that protein secretion is a fundamental mechanism through which macrophages shape the tumor microenvironment, these findings still require further validation using patient-derived cells in multicellular organoid systems and animal models. Moreover, future studies should aim to validate the potential candidate proinflammatory molecules identified in this study that are responsible for the pSTAT3-mediated downregulation of MPG and MGMT.

Methods

Cell cultures, conditioned media from differentiated macrophages, and Patient-derived GBM samples

A172 and T98G GBM cell lines (ATCC# CRL-1620, CRL-1690) were maintained in DMEM and MEM, respectively, with 10% FBS and 1% penicillin-streptomycin, while the culture medium of THP-1 monocytes (ATCC# TIB-202) was RPMI 1640 with 10% FBS, 2 mM L-glutamine, 50 μM 2-mercaptoethanol, and 1% penicillin-streptomycin. All cell lines were cultured at 37 °C in a 5% CO2 atmosphere. Suppression of STAT3 activation-phosphorylation was achieved using Stattic (ab120962, Abcam) according to the manufacturer's instructions. This selective STAT3 inhibitor blocks activation-phosphorylation, as well as subsequent dimerization and nuclear translocation of STAT3, by interacting with the SH2 domain. For macrophage differentiation, THP-1 cells were treated with 160 nM PMA (Sigma-Aldrich) for 48 h, followed by culture in RPMI with 5% FBS for 24 h. Macrophages were then polarized into M1 phenotype using IFN-γ (10 U/ml) and LPS (100 ng/ml), and into M2 using IL-13 (20 ng/ml) and IL-4 (20 ng/ml). After 24 h differentiation conditioned media (CM) was collected, centrifuged, and stored at -20 °C until use.

Tumor tissue samples were collected from 15 patients diagnosed with GBM by the Neurology, Neurosurgery, and Oncology departments of the General University Hospital of Albacete (Spain). Written informed consent was obtained from all patients in accordance with the 1964 Declaration of Helsinki and its later amendments, and all procedures were approved by the Human Ethics Committee of this hospital (Ethical approval number: 03/2014). Sociodemographic and clinical information was obtained from the hospital information system, including the date of diagnosis, surgery, cause of death (if applicable), type of antitumor therapy, and disease-free period (DFP). After collection, fresh tissue samples were homogenized in detergent lysis buffer (RIPA, Merck) for Western blot analysis.

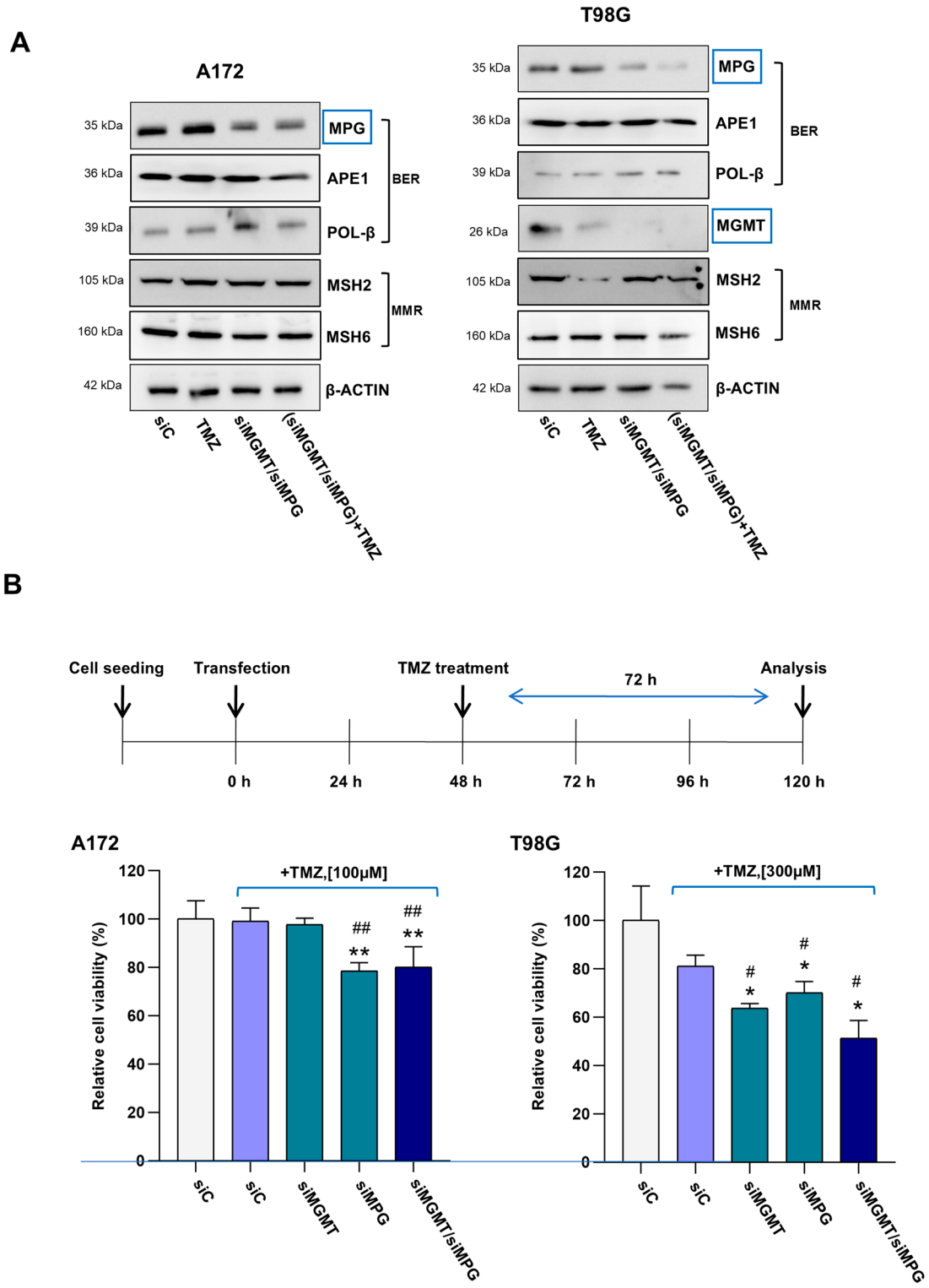

Cell viability and apoptosis assays

The MTT assay was used to assess cell viability according to the manufacturer's protocol. A172 and T98G cells were plated in 24-well plates and cultured in 500 µL of medium containing the specified concentration of TMZ. After 72 h, MTT solution (5 mg/mL) was added and incubated for 1 h at 37 °C. The medium was then removed, and a solubilizing solution was added to dissolve the formazan crystals. Absorbance was measured at 570 nm using a microplate reader (SPECTROstar Omega, BMG LABTECH), with each sample analyzed in triplicate.

Apoptosis was assessed by flow cytometry after 24 h of CM-M1 or CM-M0 treatment followed by 72 h of TMZ exposure or DMSO-vehicle control. Cells were resuspended in 450 µL of 1X Annexin V binding buffer (Immunostep) and stained with 10 µL of Annexin V conjugated to the fluorochrome Dy-634 (Immunostep), together with 40 µL of the vital dye propidium iodide (PI) (10 mg/mL, Invitrogen). Staining was performed for 1 h in the dark and analyzed using a FACS Canto II flow cytometer. Early apoptotic cells (Annexin V-positive and

◂**Fig. 6 Please make sure that Figure 6 is placed in the manuscript close to the Results section [Increased GBM chemosensitivity through MPG silencing, both alone and synergistically with MGMT downregulation], where it is cited, as we have seen in the PDF-proof that it is currently located in the Discussion section** . siRNA targeting of MPG, alone or with MGMT knockdown, potentiates TMZ efficacy. (**A**) GBM cells were transfected with scrambled (siC) or double siMGMT and siMPG for 48 h, followed by TMZ treatment for 72 h, as shown in the schematic protocol. Expression of repair enzymes was detected by Western blot analysis (representative image from three experiments), with β-actin as a loading control (original blots are presented in supplementary material: Figure s8). (**B**) The cytotoxic effect of TMZ was assessed by MTT assay in A172 and T98G cells transfected with siRNAs (siC, siMGMT, siMPG, or siMGMT/siMPG) following exposure to TMZ or vehicle. Cell viability was normalized to siC-untreated cells (100%) (mean ± SD, $n = 3$). Kruskal-Wallis test: $^{*}p < 0.05$ or $^{**}p < 0.01$ versus siC-untreated; $\#p < 0.05$ or $\#\#p < 0.01$ versus siC/TMZ-treated.

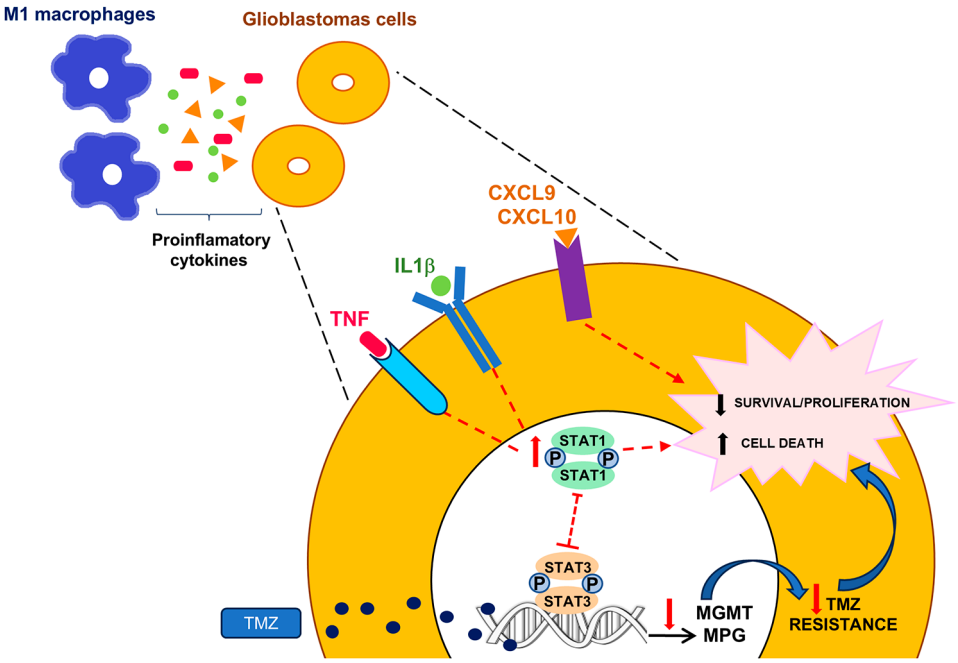

Fig. 7. This figure depicts a new mechanism by which the M1 macrophage secretome, likely via proinflammatory cytokines (TNF, IL-1β) and chemokines (CXCL9, CXCL10), downregulates DNA repair enzymes, leading to decreased resistance to TMZ. The process is mediated by the inhibition of STAT3 activation, probably driven by elevated phosphorylated STAT1.

PI-negative events), late apoptotic cells (Annexin V-positive and PI-positive events) and necrotic cells (Annexin V-negative and PI-positive events) were quantified. Additionally, caspase-3 cleavage was analyzed by Western blot as a complementary measure of apoptosis.

To evaluate the effect of macrophage-conditioned medium (CM) on GBM cells, A172 and T98G cells were treated with CM for 24 h, followed by 72 h with or without TMZ. Viability (MTT assay) and apoptosis (flow cytometry and Western blot) were measured.

Western blot analysis

Proteins from cell culture and tumor tissue homogenates were extracted using RIPA buffer, and protein concentration was determined by the BCA assay. Protein extracts (30–40 µg) were separated on denaturing SDD-PAGE polyacrylamide gels and transferred to a PVDF membrane (Hybond-C Extra, Amersham Biosciences). Spectra™ Multicolor Broad Range Protein ladder (Thermo Scientific #26634) was used as a molecular weight marker for protein size estimation. The following primary antibodies were used: anti-MGMT (2739 S), anti-pSTAT3 (D3A7), anti-pSTAT1 (58D6), anti-STAT3 (124H6), and anti-STAT1 (9172 S) from Cell Signaling, anti-MPG (sc-101237), anti-MSH2 (sc-376384), anti-APE1 (sc-17774), anti-PARP-1 (sc-8007), anti-BLC2 (sc-7382), anti-caspase-3 (sc-56053) and anti-β-ACTIN (sc-81178) from Santa Cruz, and anti-DNA polymerase (ab26343) from Abcam. Chemiluminescence detection was performed using the SuperSignal™ West Dura (Thermo Scientific) on a Luminescent Image Analyzer LAS-mini 4000 system (Fujifilm, Tokyo, Japan).

Characterization of macrophage secretomes by quantitative proteomic analysis (LC-MS/MS) using SWATH acquisition

Sample preparation: Unconditioned medium (2 replicates), M0-conditioned medium (2 replicates), and M1-conditioned medium were processed using an albumin depletion protocol as described by Nakamura et al.[48]. In the first approach, 100 µL of supernatant was mixed with 350 µL of ProMax Binding/Wash Buffer and 20 µL of ProMax magnetic particles. After gentle agitation for 20 min at room temperature, magnetic separation was performed to remove the albumin-containing supernatant. The particles were washed three times, and bound proteins were eluted using 100 mM Tris-HCl (pH 8.5) containing 2% SDS. The eluate was collected in fresh microtubes by magnetic separation. Although the manufacturer recommends protocol optimization depending on the application, no additional adjustments were required under our experimental conditions. In a second (non-depleted) approach, 5 µL of supernatant was diluted with 95 µL of the same Tris-HCl/SDS buffer.

Digestion procedure: Albumin-depleted media were digested using the Single-Pot Solid-Phase-Enhanced Sample Preparation (SP3) method, following the protocol described by Hughes et al.[49]. Samples were reduced with DTT and alkylated with IAA, then mixed with 6 µL of SP3 beads (50 µg/µL) and adjusted to 30 µL with water. Ethanol was added to a final concentration of 70% (v/v), and samples were incubated at 1,000 rpm at room temperature for 20 min. Beads were immobilized using a magnetic rack, the supernatant was discarded, and the procedure was repeated. The pellet was washed several times with 80% ethanol and then resuspended in 300 µL of 20 mM ammonium bicarbonate containing trypsin (enzyme-to-protein ratio 1:25, w/w). Digestion was carried out overnight at 37 °C and 1,000 rpm. After centrifugation at 20,000×*g*, the supernatant was collected and acidified with 2% formic acid.

LC-MS/MS (liquid chromatography-tandem mass spectrometry) analysis for library generation, *DDA*, *and SWATH acquisition*: To generate a spectral library, peptide mixtures were analyzed using a shotgun proteomics approach via microLC-MS/MS. Samples were pooled, and 1 µg was injected into an Ekspert™ nanoLC425 system (Eksigent) equipped with a Luna Omega Polar C18 column (3 µm, 0.3 × 150 mm) and a Polar C18 trap column. Mobile phases used were: (A) 0.1% formic acid, 2% acetonitrile; and (B) 98% acetonitrile, 0.1% formic acid. Peptides were desalted for 3 min and then separated using a 30-minute gradient from 6 to 30% B, followed by a rapid transition to 95% B and column re-equilibration.

Mass analysis was performed on a TripleTOF® 6600 + Q-TOF mass spectrometer (Sciex) equipped with an Optiflow MicroProbe source operated at 4.5 kV and 75 °C. In data-dependent acquisition (DDA) mode, MS1 scans (350–1400 m/z, 250 ms) were followed by MS2 scans (100–1500 m/z, 25 ms) on up to 100 precursor ions (charge states 2 + to 4+), with dynamic exclusion set to 15 s.

For SWATH acquisition, MS1 scans were followed by 25 ms fragment ion scans across 70 variable windows (350–1400 m/z), resulting in a total cycle time of 1.92 s. Sample injections were randomized to minimize batch effects.

Data analysis: Raw data files were converted to mzML format using ProteoWizard and analyzed with FragPipe for protein identification and label-free quantification[50]. Contaminant proteins, single-peptide identifications, and inconsistently quantified proteins across replicates were excluded. The data were log2-transformed, and missing values were imputed using a left-shifted Gaussian distribution (1.8 standard deviations, width = 0.3).

Differential expression analysis was conducted using linear models with empirical Bayes moderation, as implemented in the limma package (Bioconductor, R). Proteins were considered significantly differentially expressed if they exhibited an adjusted p-value < 0.05 and an absolute log2 fold change ≥ 1.5.

Gene Silencing and cell transfections

A172 and T98G cells were transfected with increasing concentrations of siRNAs (25, 40,80 nM) targeting MPG and MGMT (Santa Cruz), using siRNA Transfection Reagent (sc-29527). Briefly, cells were seeded one day prior to transfection in 6-well plates for Western blot and qRT-PCR analysis, or in 24-well plates for cell viability assessment, with 10% FBS in their respective media. The siRNA-transfection reagent complex was prepared in transfection medium (sc-36868, Santa Cruz) according to the manufacturer's instructions. The medium was replaced with fresh medium 8 h after transfection. After a minimum of 48 h, protein extracts were prepared for Western blot and qRT-PCR analysis. Cell viability was assessed after an additional 72-hour TMZ treatment.

For plasmid transfections, A172 and T98G cells were seeded in 6-well plates and transfected 24 h later with Lipofectamine 2000 (Invitrogen) according to the manufacturer's instructions, using OPTI-MEM medium (Gibco) and 2.5 µg of total plasmid DNA (pCMV-Sport6, pCMV-Sport6-STAT1, or pCMV-Sport6-STAT3) per well. Cells were analyzed 24 h post-transfection.

RNA isolation and qRT-PCR analysis

Total RNA was extracted using the RNA Total Isolation Kit (Nzytech) and converted into cDNA using RevertAid™ Minus First Strand (Thermo Scientific). Gene expression was analyzed using SYBR™ Green PCR Master Mix (Applied Biosystems). Primers used included the following sequences:

MGMT:
Forward: 5′-GTCGTTCACCAGACAGGTGTTA-3′;
Reverse: 5′-ACAGGATTGCCTCTCATTGCTC-3′.
MPG:
Forward:5′-TTGGAGTTCTTCGACCAGCC-3′;
Reverse: 5′-CATGAACATGCCTCGGTTGC-3′.
β-actin:
Forward:5′-AAGATCATTGCTCCTCCTG-3′;
Reverse: 5′-CGTCATACTCCTGCTTGCTG-3′.

Statistical analysis

Data were analyzed using IBM SPSS Statistics 22. Statistical significance was evaluated with Student's t-test, Mann-Whitney U test for two-group comparisons, and one-way ANOVA with Dunnett's post-hoc test for multiple comparisons.

Data availability

Data is provided within the manuscript or supplementary information files.

Received: 9 February 2025; Accepted: 30 September 2025
Published online: 06 November 2025

References

1. Grochans, S. et al. Epidemiology of glioblastoma multiforme–Literature review. *Cancers (Basel)* **14**, 2412. https://doi.org/10.3390/cancers14102412 (2022).
2. Stupp, R. et al. Radiotherapy plus concomitant and adjuvant temozolomide for glioblastoma. *N. Engl. J. Med.* **352**, 987–996. https://doi.org/10.1056/NEJMoa043330 (2005).
3. Andersen, J. K., Miletic, H. & Hossain, J. A. Tumor-associated macrophages in Gliomas—Basic insights and treatment opportunities. *Cancers (Basel)* **14**, 1319. https://doi.org/10.3390/cancers14051319 (2022).
4. Mantovani, A. & Allavena, P. The interaction of anticancer therapies with tumor-associated macrophages. *J. Exp. Med.* **212**, 435–445. https://doi.org/10.1084/jem.20150295 (2015).
5. Zhang, Y. et al. Overexpression of STAT1 suppresses angiogenesis under hypoxia by regulating VEGF–A in human glioma cells. *Biomed. Pharmacother.* **104**, 566–575. https://doi.org/10.1016/j.biopha.2018.05.079 (2018).
6. Kim, H. S. & Lee, M. S. STAT1 as a key modulator of cell death. *Cell. Signal.* **19**, 454–465. https://doi.org/10.1016/j.cellsig.2006.09.003 (2007).
7. Han, Z. et al. Silencing of the STAT3 signaling pathway reverses the inherent and induced chemoresistance of human ovarian cancer cells. *Biochem. Biophys. Res. Commun.* **435**, 188–194. https://doi.org/10.1016/j.bbrc.2013.04.087 (2013).
8. Jiang, Y. et al. STAT1 mediates transmembrane TNF-alpha-induced formation of death-inducing signaling complex and apoptotic signaling via TNFR1. *Cell. Death Differ.* **24**, 660–671. https://doi.org/10.1038/cdd.2016.162 (2017).
9. Ge, Y. et al. Interactions between tumor-associated macrophages and regulated cell death: Therapeutic implications in immuno-oncology. *Front. Oncol.* **14**, 1449696. https://doi.org/10.3389/fonc.2024.1449696 (2024).
10. Binabaj, M. et al. The prognostic value of MGMT promoter methylation in glioblastoma: A meta-analysis of clinical trials. *J. Cell. Physiol.* **233**, 378–386. https://doi.org/10.1002/jcp.25896 (2018).
11. Serrano-Heras, G. et al. Involvement of N-methylpurine DNA glycosylase in resistance to temozolomide in patient-derived glioma cells. *Sci. Rep.* **10**, 22185. https://doi.org/10.1038/s41598-020-78868-0 (2020).
12. Agnihotri, S. et al. Alkylpurine–DNA–N-glycosylase confers resistance to temozolomide in xenograft models of glioblastoma multiforme and is associated with poor survival in patients. *J. Clin. Invest.* **122**, 253–266. https://doi.org/10.1172/JCI59334 (2012).
13. Montaldi, A. P. & Sakamoto-Hojo, E. T. Methoxyamine sensitizes the resistant glioblastoma T98G cell line to the alkylating agent temozolomide. *Clin. Exp. Med.* **13**, 279–288. https://doi.org/10.1007/s10238-012-0201-x (2013).
14. Barazzuol, L. et al. Evaluation of poly (ADP-ribose) polymerase inhibitor ABT-888 combined with radiotherapy and temozolomide in glioblastoma. *Radiat. Oncol.* **8**, 65. https://doi.org/10.1186/1748-717X-8-65 (2013).
15. Li, J. et al. Overcoming temozolomide resistance in glioblastoma via enhanced NAD + Bioavailability and Inhibition of Poly-ADP-Ribose glycohydrolase. *Cancers (Basel)* **14**, 3572. https://doi.org/10.3390/cancers14153572 (2022).
16. Kohsaka, S. et al. STAT3 Inhibition overcomes temozolomide resistance in glioblastoma by downregulating MGMT expression. *Mol. Cancer Ther.* **11**, 1289–1299. https://doi.org/10.1158/1535-7163.MCT-11-0801 (2012).
17. Wang, X. et al. Gain of function of mutant TP53 in glioblastoma: Prognosis and response to Temozolomide. *Ann. Surg. Oncol.* **21**, 1337–1344. https://doi.org/10.1245/s10434-013-3380-0 (2014).
18. Schust, J., Sperl, B., Hollis, A., Mayer, T. U. & Berg, T. Stattic: A small-molecule inhibitor of STAT3 activation and dimerization. *Chem. Biol.* **13**, 1235–1242. https://doi.org/10.1016/j.chembiol.2006.09.01 (2006).
19. Wang, Y. et al. The IL-1β/STAT1 axis inhibits STAT3 function via sequestration of the transcriptional activator GLIS2, leading to postoperative vascular dysfunction. *Int. Immunopharmacol.* **143**, 113372. https://doi.org/10.1016/j.intimp.2024.113372 (2024).
20. Flood, B. et al. Caspase-11 regulates the tumour suppressor function of STAT1 in a murine model of colitis-associated carcinogenesis. *Oncogene* **38**, 2658–2674. https://doi.org/10.1038/s41388-018-0613-5 (2019).
21. Liu, M., Guo, S. & Stiles, J. K. The emerging role of CXCL10 in cancer (Review). *Oncol. Lett.* **2**, 583–589. https://doi.org/10.3892/ol.2011.300 (2011).
22. Chan, T. Y. H., Wong, J. S. Y., Kiang, K. M. Y., Sun, C. W. Y. & Leung, G. K.-K. The duality of CXCR3 in glioblastoma: Unveiling autocrine and paracrine mechanisms for novel therapeutic approaches. *Cell. Death Dis.* **14**, 835. https://doi.org/10.1038/s41419-023-06354-2 (2023).
23. Kang, M. et al. Multiple functions of Fubp1 in cell cycle progression and cell survival. *Cells* **9**, 1347. https://doi.org/10.3390/cells9061347 (2020).
24. Huang, B., Yuan, Q., Sun, J., Wang, C. & Yang, D. Thymidine phosphorylase in nucleotide metabolism: Physiological functions and its implications in tumorigenesis and anti-cancer therapy. *Front. Immunol.* **16**, 1561560. https://doi.org/10.3389/fimmu.2025.1561560 (2025).
25. Mantovani, A., Schioppa, T., Porta, C., Allavena, P. & Sica, A. Role of tumor-associated macrophages in tumor progression and invasion. *Cancer Metastasis Rev.* **25**, 315–322. https://doi.org/10.1007/s10555-006-9001-7 (2006).
26. Wei, J. et al. Immune biology of glioma-associated macrophages and microglia: Functional and therapeutic implications. *Neuro Oncol.* **22**, 180–194. https://doi.org/10.1093/neuonc/noz212 (2020).
27. Singh, N., Miner, A., Hennis, L. & Mittal, S. Mechanisms of Temozolomide resistance in glioblastoma—a comprehensive review. *Cancer Drug Resist.* **4**, 17–43. https://doi.org/10.20517/cdr.2020.79 (2021).
28. Shao, Y., Han, S., Hou, Z., Yang, C. & Zhao, Y. Tumor-associated macrophages within the immunological milieu: An emerging focal point for therapeutic intervention. *Heliyon* **10**, e36839. https://doi.org/10.1016/j.heliyon.2024.e36839 (2024).
29. Song, W., Thakor, P., Vesey, D. A., Gobe, G. C. & Morais, C. Conditioned medium from stimulated macrophages inhibits growth but induces an inflammatory phenotype in breast cancer cells. *Biomed. Pharmacother.* **106**, 247–254. https://doi.org/10.1016/j.biopha.2018.06.126 (2018).
30. Chai, D. et al. Absent in melanoma 2-mediating M1 macrophages facilitate tumor rejection in renal carcinoma. *Transl Oncol.* **14**, 101018. https://doi.org/10.1016/j.tranon.2021.101018 (2021).
31. Lentilhas-Graça, J. et al. The secretome of macrophages has a differential impact on spinal cord injury recovery according to the polarization protocol. *Front. Immunol.* **15**, 1354479. https://doi.org/10.3389/fimmu.2024.1354479 (2024).
32. Zhu, Y. et al. A comprehensive proteomics analysis reveals a secretory path- and status-dependent signature of exosomes released from tumor-associated macrophages. *J. Proteome Res.* **14**, 4319–4331. https://doi.org/10.1021/acs.jproteome.5b00770 (2015).

33. Zhao, L. et al. Critical roles of chemokine receptor CCR5 in regulating glioblastoma proliferation and invasion. *Acta Biochim. Biophys. Sin. (Shanghai)* **47**, 890–898. https://doi.org/10.1093/abbs/gmv095 (2015).
34. Signoret, N. et al. Agonist-induced endocytosis of CC chemokine receptor 5 is clathrin dependent. *Mol. Biol. Cell.* **16**, 902–917. https://doi.org/10.1091/mbc.e04-08-0687 (2005).
35. Hegi, M. E. et al. Correlation of O6-methylguanine methyltransferase (MGMT) promoter methylation with clinical outcomes in glioblastoma and clinical strategies to modulate MGMT activity. *J. Clin. Oncol.* **26**, 4189–4199. https://doi.org/10.1200/JCO.2007.11.5964 (2008).
36. Liu, C. et al. Aberrant expression of N-methylpurine-DNA glycosylase influences patient survival in malignant gliomas. *J. Biomed. Biotechnol.* 760679. https://doi.org/10.1155/2012/760679 (2012).
37. Agnihotri, S. et al. ATM regulates 3-methylpurine-DNA glycosylase and promotes therapeutic resistance to alkylating agents. *Cancer Discov.* **4**, 1198–1213. https://doi.org/10.1158/2159-8290.CD-14-0157 (2014).
38. Fishel, M. L., He, Y., Smith, M. L. & Kelley, M. R. Manipulation of base excision repair to sensitize ovarian cancer cells to alkylating agent temozolomide. *Clin. Cancer Res.* **13**, 260–267. https://doi.org/10.1158/1078-0432.CCR-06-1920 (2007).
39. Fosmark, S. et al. APNG as a prognostic marker in patients with glioblastoma. *PLOS One* **12**, e0178693. https://doi.org/10.1371/journal.pone.0178693 (2017).
40. Tang, J. et al. N-methylpurine DNA glycosylase and DNA polymerase β modulate BER inhibitor potentiation of glioma cells to Temozolomide. *Neuro Oncol.* **13**, 471–486. https://doi.org/10.1093/neuonc/nor01 (2011).
41. Mathewson, N. D. et al. Inhibitory CD161 receptor identified in glioma-infiltrating T cells by single-cell analysis. *Cell* **184**, 1281–1298.e26. https://doi.org/10.1016/j.cell.2021.01.022 (2021).
42. Domingues, P. et al. Tumor infiltrating immune cells in gliomas and meningiomas. *Brain Behav. Immun.* **53**, 1–15. https://doi.org/10.1016/j.bbi.2015.07.019 (2016).
43. Fujiwara, Y., Komohara, Y., Ikeda, T. & Takeya, M. Corosolic acid inhibits glioblastoma cell proliferation by suppressing the activation of signal transducer and activator of transcription-3 and nuclear factor-kappa B in tumor cells and tumor-associated macrophages. *Cancer Sci.* **102**, 206–211. https://doi.org/10.1111/j.1349-7006.2010.01772.x (2011).
44. Genard, G., Lucas, S. & Michiels, C. Reprogramming of tumor-associated macrophages with anticancer therapies: radiotherapy versus chemo- and immunotherapies. *Front. Immunol.* **8**, 828. https://doi.org/10.3389/fimmu.2017.00828 (2017).
45. Yan, T. et al. Suppression of the hyaluronic acid pathway induces M1 macrophages polarization via STAT1 in glioblastoma. *Cell. Death Discov.* **8**, 1–13. https://doi.org/10.1038/s41420-022-00973-y (2022).
46. Ranson, M. et al. Lomeguatrib, a potent inhibitor of O6-Alkylguanine-DNA-Alkyltransferase: Phase I Safety, Pharmacodynamic, and Pharmacokinetic trial and evaluation in combination with Temozolomide in patients with advanced solid tumors. *Clin. L Cancer Res.* **12**, 1577–1584. https://doi.org/10.1158/1078-0432.CCR-05-2198 (2006).
47. Quinn, J. A. et al. Phase II trial of temozolomide plus O6-benzylguanine in adults with recurrent, temozolomide-resistant malignant glioma. *J Clin. Oncol.* 27, 1262–1267. https://doi.org/10.1200/JCO.2008.18.8417 (2009).
48. Nakamura, R. et al. A simple method for in-depth proteome analysis of mammalian cell culture conditioned media containing fetal bovine serum. *Int. J. Mol. Sci.* **22**, 2565. https://doi.org/10.3390/ijms22052565 (2021).
49. Hughes, C. S. et al. Ultrasensitive proteome analysis using paramagnetic bead technology. *Mol. Syst. Biol.* **10**, 757. https://doi.org/10.15252/msb.20145625 (2014).
50. Yu, F. et al. Analysis of DIA proteomics data using MSFragger-DIA and FragPipe computational platform. *Nat. Commun.* **14**, 4154. https://doi.org/10.1038/s41467-023-39869-5 (2023).

Acknowledgements

We would like to express our deepest gratitude to the patients who participated in this study and generously donated tumor samples. The authors also wish to acknowledge Dr. Jaime Gallego Pérez de Larraya, Coordinator of the Neuro-Oncology Area at Clínica Universidad de Navarra, Spain, for his valuable advice and ongoing support throughout the development of this line of research. Proteomic analyses were performed at the Proteomics Unit of Hospital Nacional de Parapléjicos, Toledo, Spain, whose technical support and expertise are gratefully acknowledged.

Author contributions

S.L., MJM.D., T.S and G.S provided conception. S.L., B.C., N.G., MJM.D., L.A., RA.B. and G.S. conducted experiments and curated data. S.L., B.C., N.G., MJM.D., L.A., H.S., D.G., CJ.K., RA.B., T.S. and G.S. analyzed the results. H.S., D.G. and CJ.K. performed patient inclusion and collected human samples. S.L., T.S., and G.S. wrote the initial manuscript draft and prepared the revised version. T.S. and G.S. acquired funding and supervised the study. All authors reviewed the revised manuscript.

Funding

Susana López-López was the recipient of a contract funded by Fundación Hospital Nacional de Parapléjicos- Instituto de Investigación Sanitaria de Castilla-La Mancha (IDISCAM), Castilla-La Mancha, Spain, during the years 2021 and 2022. Gemma Serrano-Heras is the recipient of a contract funded by the grant awarded to the project ´ Refuerzo de la actividad investigadora de Castilla-La Mancha (EMER)´ (Fundación Hospital Nacional de Parapléjicos- Instituto de Investigación Sanitaria de Castilla-La Mancha (IDISCAM), Castilla-La Mancha, Spain).

Declarations

Competing interests

The authors declare no competing interests.

Ethical approval

for all study protocols has been obtained from the Human Ethics Committee of the General University Hospital of Albacete, Spain (Ethical approval number: 03/2014). This study adheres to the Declaration of Helsinki ethical principles for medical research involving human subjects, including its amendments.

Additional information

Supplementary Information The online version contains supplementary material available at https://doi.org/10.1038/s41598-025-22674-z.

Correspondence and requests for materials should be addressed to T.S. or G.S.-H.

Reprints and permissions information is available at www.nature.com/reprints.

Publisher's note Springer Nature remains neutral with regard to jurisdictional claims in published maps and institutional affiliations.